Clays and Clay Minerals, Vol. 61, No. 6, 525–531, 2013.

HYDROTHERMAL SYNTHESIS OF MESOPOROUS MAGADIITE PLATES *VIA* HETEROGENEOUS NUCLEATION

YALU MA*, NA LIU, XIAONING JIN, AND TIANSHI FENG

Department of Chemistry, Institute of Science, Tianjin University, Tianjin 300072, China

Abstract—The conventional cauliflower-like shape of magadiite imposes serious limitations on its applications in adsorption, catalysis, ion exchange, *etc*. To overcome this problem, a method to prepare it with plate-like structures was developed. This novel approach is based on an interface-controlled heterogeneous nucleation process. Zirconia grinding balls with diameters of 2.0 mm were dispersed in the starting solution to provide solid−liquid interfaces. Then the starting solution with a SiO_2:NaOH:H_2O molar ratio of 9:2:75 was subjected to hydrothermal treatment at 433 K for 96 h. The presence of the solid−liquid interface improved the crystallization yield and controlled the morphology and specific surface area of the crystals. With the zirconia balls, the yield and sizes of the plate-like magadiite were 52 wt.% and 1−3 μm, respectively. In the absence of zirconia balls, the yield was smaller (45 wt.%) and magadiite shaped like cauliflower was formed. The plate-like magadiite had a specific surface area of 66 $m^2\ g^{-1}$ and a pore-size distribution between 4 and 5 nm, compared with a surface area of 28 $m^2\ g^{-1}$ for the cauliflower-like magadiite. In addition, the plate-like magadiite was a more effective ion exchanger than the cauliflower-like magadiite with a cation exchange capacity of 64.5 mmol/100 g (compared to 53.8 mmol/100 g for the cauliflower-like form) and it had a faster sorption rate for calcium ions.

Key Words—Ca^{2+} Adsorption, Cauliflower-like Magadiite, Heterogeneous Nucleation, Hydrothermal Reaction, Plate-like Magadiite.

INTRODUCTION

Magadiite ($Na_2Si_{14}O_{29}{\cdot}xH_2O$) belongs to the family of hydrous sodium silicate minerals which also includes kanemite, makatite, kenyaite, and octosilicate (Almond *et al*., 1997; Huang *et al*., 1999). Magadiite was first described by Beugster (1967) who discovered it, together with kenyaite, in lake beds in Lake Magadi in Kenya. Magadiite has a layered structure with negatively charged silicate layers. The silicon atoms are tetrahedrally coordinated to four oxygen atoms, with sodium ions in the interlayer spaces. Due to the presence of the Na^+ ions, water molecules, and silanol groups in the interlayer spaces, several derivative compounds of magadiite have been prepared through interlayer grafting, silylation, and pillaring reactions (Mallouk and Gavin, 1988; Takahashi and Kuroda, 2011). Recent studies of magadiite have mainly focused on adsorption (Guerra *et al*., 2010; Ide *et al*., 2011; Nunes *et al*., 2011), cation exchange (Eypert-Blaison *et al*., 2002; Supronowicz *et al*., 2012; Chen *et al*., 2013), intercalation (Ágnes *et al*., 1999; Pastore *et al*., 2000; Kooli *et al*., 2006), and modification (Zhang *et al*., 2003; Díaz *et al*., 2007; Macedo *et al*., 2007).

Although magadiite is found in nature, it can also be synthesized under hydrothermal conditions using commercial silicas, such as silica gel, silica powder, and colloidal silica. Production costs, however, are high and these need to be reduced in order for synthetic magadiite to become practical for conventional industrial applications. A route for synthesizing magadiite that uses a sodium silicate solution and fluorosilicic acid (H_2SiF_6) was reported by Kwon and Park (2004). Rosette-like magadiite was prepared using water glass as the silicon source and a hydrothermal reaction at 423 K (Wang *et al*., 2006). The use of sodium silicate or water glass as the silica source could reduce production costs as both of these materials are inexpensive.

The present study reports a novel process to prepare plate-like magadiite by heterogeneous nucleation at a solid–liquid interface. Commercially available zirconia balls were dispersed in a sodium silicate solution to form solid–liquid interfaces. The ball-containing solution was then subjected to a static hydrothermal reaction. The effects of the presence or absence of zirconia balls on the magadiite crystallization process and crystalline forms were studied by scanning electron microscopy (SEM), transmission electron microscopy (TEM), N_2 adsorption, infrared (IR) spectroscopy, and X-ray diffraction (XRD). The cation exchange capacity (CEC) of Ca^{2+} was also investigated using the synthesized magadiite.

EXPERIMENTAL

Materials

The raw material was a commercially available aqueous sodium silicate solution (also known as water glass, 26 wt.% SiO_2, 8.2 wt.% NaOH, molar ratio of SiO_2/Na_2O = 3.3, Tianjin Hui Da Cheng Chemical Co., Ltd., China) and a silica sol (30 wt.% SiO_2, Qingdao

* E-mail address of corresponding author:
mayalutju@126.com
DOI: 10.1346/CCMN.2013.0610605

Ocean Chemical Co., Ltd., China). The zirconia grinding balls (5% yttria-stabilized) with a mean diameter of 2 mm were purchased from Jiangsu Grand Advanced Ceramics Co., Ltd, China. Calcium chloride ($CaCl_2$) with 99% purity was obtained from Tianjin Chemical Reagent Co., China, and was used without further purification to prepare a standard Ca^{2+} stock solution of 300 mg L^{-1}. Distilled water was used throughout the study.

Preparation of magadiite

Magadiites were prepared in an aqueous solution with a SiO_2:NaOH:H_2O molar ratio of 9:2:75, the optimal ratio reported by Lagaly and Beneke (1975). In short, 14 g of water glass and 10 mL of deionized water were stirred in a water bath at 333 K for 1 h and then 21 g of silica sol was added dropwise to the solution and stirring was continued for another 5 h. Checks were made using pH indicator strips to ensure the pH was maintained at 12.0. The solution was then transferred to a Teflon-lined cylindrical reactor, sealed, and reacted hydrothermally under static conditions at 433 K for 4−120 h. The pressure in the autoclave was maintained at the equilibrium pressure at 433 K. In order to form solid−liquid interfaces in the solution, yttria-stabilized zirconia grinding balls were added to the solution prior to the start of the hydrothermal process. With the presence or absence of zirconia balls, two different kinds of magadiites were formed during hydrothermal crystalline reaction.

After synthesis, the autoclave was cooled to room temperature. The dispersion was then centrifuged for 5 min with a single-bearing centrifuge at $2800 \times g$. The separated solid product was washed several times with deionized water and vacuum-dried in air at 373 K for 12 h. The yields of magadiites for the different periods of hydrothermal treatment (4−120 h) were defined as the mass ratio of dried sample to the maximum theoretical amount of magadiite that could be formed from 45 g of starting solution. At least three replicates were performed for each measurement. The reported yields are the mean values of several measurements.

Physical measurements

Scanning electron microscopy images were recorded for the samples using a Nanosem-430 scanning electron microscope (FEI Corp., Hillsboro, Oregon, USA). Energy dispersive X-ray spectroscopy (EDS) was used to confirm the atomic compositions of the samples and to reveal any contamination from the zirconia balls. The sample prepared with the zirconia balls was deposited on a carbon-coated copper mesh from an ethanol dispersion and high-resolution transmission electron microscopy (HRTEM) images were collected using a Tecncai G2 F20 transmission electron microscope (FEI Corp., Eindhoven, The Netherlands) at an accelerating voltage of 200 kV. Selected area electron diffraction (SAED) patterns were then recorded to identify the crystal structure. Infrared spectra (Nicolet 6700, Thermo Fisher Scientific Inc., Waltham, Massachusetts, USA) of the samples were obtained in KBr pellets; the powdered samples were combined with infrared-grade KBr powder at a ratio of 2:180 mg. The XRD measurements (D/max-2500, Rigaku Corp., Tokyo, Japan) were collected at a tube voltage of 40 kV and a tube current of 200 mA using CuKα radiation (λ = 1.5406 Å), at a scanning rate of 0.02° s^{-1} from the 2θ range of 1 to 80°. The N_2 adsorption-desorption isotherms were obtained using a NOVA 2000 instrument (Quantachrome Corp., Boynton Beach, Florida, USA) at 77 K. Specific surface areas were calculated using the Brunauer-Emmet-Teller (BET) method and pore-size distributions were calculated using the Barrett-Joyner-Halenda (BJH) method.

Adsorption of calcium ions

Adsorption studies were performed by adding 0.2 g of sorbent (magadiite) to 100 mL of 300 mg L^{-1} Ca^{2+} aqueous solution (pH = 7) in a capped conical flask. The mixture was then agitated for t min (t = 2, 6, 10, 20, 30, 50, 70, 90, 110, 130, 150, or 170) in a temperature-controlled water bath shaker (SHZ-88, Shanghai, China) at 298 K. At time t, the supernatant was removed and filtered, and the Ca^{2+} concentration in each flask was determined using an atomic absorption spectrophotometer (AAS) (180-80, Hitachi, Japan). The adsorption capacity of Ca^{2+} at a given time (q_t (mg g^{-1})) was calculated as follows:

$$q_t = (C_0 - C_t)V/W$$

where C_0 is the initial Ca^{2+} concentration (mg L^{-1}); C_t is the Ca^{2+} concentration measured by AAS at time t (mg L^{-1}); V is the volume of the solution (L); and W is the weight of the sorbent (g).

The CEC of Ca^{2+} (mmol/100 g) was calculated using:

$$CEC = (q_{max} \times 100)/M_{Ca}$$

where q_{max} is the maximum adsorption capacity of Ca^{2+} (mg g^{-1}) at equilibrium and M_{Ca} is the molar mass of Ca^{2+}, 40 g mol^{-1}.

RESULTS AND DISSCUSSION

The effect of the zirconia balls on the crystallization of magadiite was investigated by adding 250 zirconia balls with diameters of 2 mm (Figure 1a, total solid volume of 1 mL) to the hydrothermal sodium silicate synthesis solution. These balls provided constant solid−liquid interfacial areas in the solution. The zirconia balls had a significant effect on the crystallization process. With no zirconia balls, the magadiite formed was the conventional cauliflower-type (C-magadiite) and with the zirconia balls the magadiite formed was plate-like in form (P-magadiite). The yields

https://doi.org/10.1346/CCMN.2013.0610605 Published online by Cambridge University Press

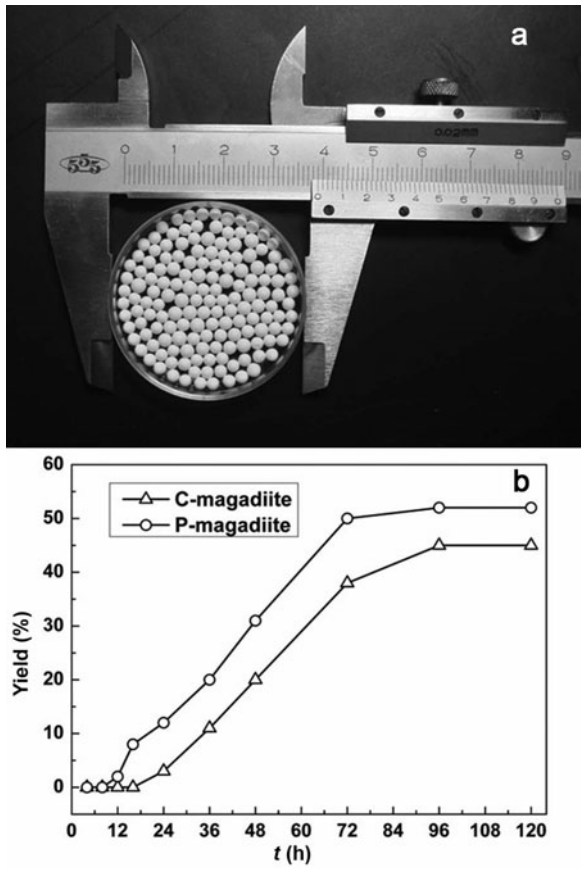

Figure 1. (a) Zirconia balls with a diameter of 2.0 mm and (b) yields of magadiite *vs.* hydrothermal reaction time at 433 K.

of both C- and P-magadiite (Figure 1b) increased with hydrothermal treatment though greater yields were obtained for P-magadiite. In the presence of the zirconia balls, the yield started to increase after ~12 h and the equilibrium and maximum yields were reached after 72 h; the yield was ~52% of theoretical yield. When zirconia balls were not used, yield started to increase after 16 h and the maximum yield of ~45% was not reached until after 96 h.

Analysis by XRD was used to confirm that the products obtained with and without the zirconia balls during the hydrothermal treatment at 433 K were in fact magadiite. The XRD patterns of both the magadiites prepared (Figure 2) showed a d_{001} reflection corresponding to a basal spacing of 15.6 Å. This interlayer spacing is in agreement with the literature value of 15.5 Å, corresponding to the d_{001} reflection peak of Na-magadiite (Eypert-Beneke *et al.*, 2001), and all the reflections could be indexed to magadiite peaks based on the information provided by Schwieger and Lagaly (2004). The XRD patterns and chemical analysis of the samples synthesized were also in agreement with JCPDS 42-1350 for single-phase Na-magadiite.

In general terms, SEM provides information about the morphology and TEM identifies the internal structure of

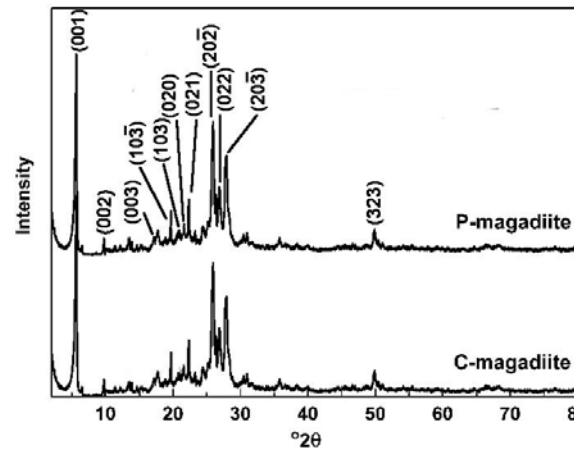

Figure 2. XRD patterns of C- and P-magadiite synthesized hydrothermally at 433 K for 96 h.

the layered crystals. The SEM and TEM images of the magadiites prepared with and without zirconia balls by hydrothermal synthesis at 433 K for 96 h are shown in Figure 3. In the absence of zirconia balls, the C-magadiite particles (Figure 3a,b) were shaped like cauliflower with the diameters of the 'flowers' and 'petals' of ~10−20 and 3−5 μm, respectively. This cauliflower-like morphology is typical and similar to images given in the literature (Kooli *et al.*, 2006; Kikuta *et al.*, 2002). Conventional magadiite powder has been reported to have 'cauliflower' or 'rosette' morphology, consisting of aggregates of thin platelets with diameters of ~10−20 μm. In the presence of the zirconia balls, the P-magadiite (Figure 3c) showed isolated plate-like morphology. The size of the plates was ~1−3 μm. The SEM-EDS compositional analyses of the point marked with a cross in Figure 3c shows that the Na:Si:O atom ratio was ~4.44:27.75:67.81 for the P-magadiite (Figure 3d). This is in good agreement with the approximate composition of $Na_2Si_{14}O_{29}{\cdot}xH_2O$ suggested by Zhang *et al.* (2003). In addition, EDS analysis of the two magadiite samples showed that the level of impurities in the sample prepared with zirconia balls was almost the same as that for the sample prepared without the balls. The samples were, therefore, not contaminated by the zirconia balls during the hydrothermal process.

Selected area electron diffraction coupled with HRTEM constitutes a powerful tool for analyzing the crystalline structure in the layers. The magadiite sample prepared with zirconia balls shows a typical morphology for thin tetragonal platelets (Figure 3e) and the SAED pattern (Figure 3f) indicates a highly crystalline material. The SAED pattern belongs to the tetragonal *I*41/*amd* space group, and the crystalline structure was confirmed by the XRD data (Figure 2). The decrease in the symmetry of the electron diffraction spots under the electron beam is probably due to the migration of the Na cations and the lack of structural stability in the

https://doi.org/10.1346/CCMN.2013.0610605 Published online by Cambridge University Press

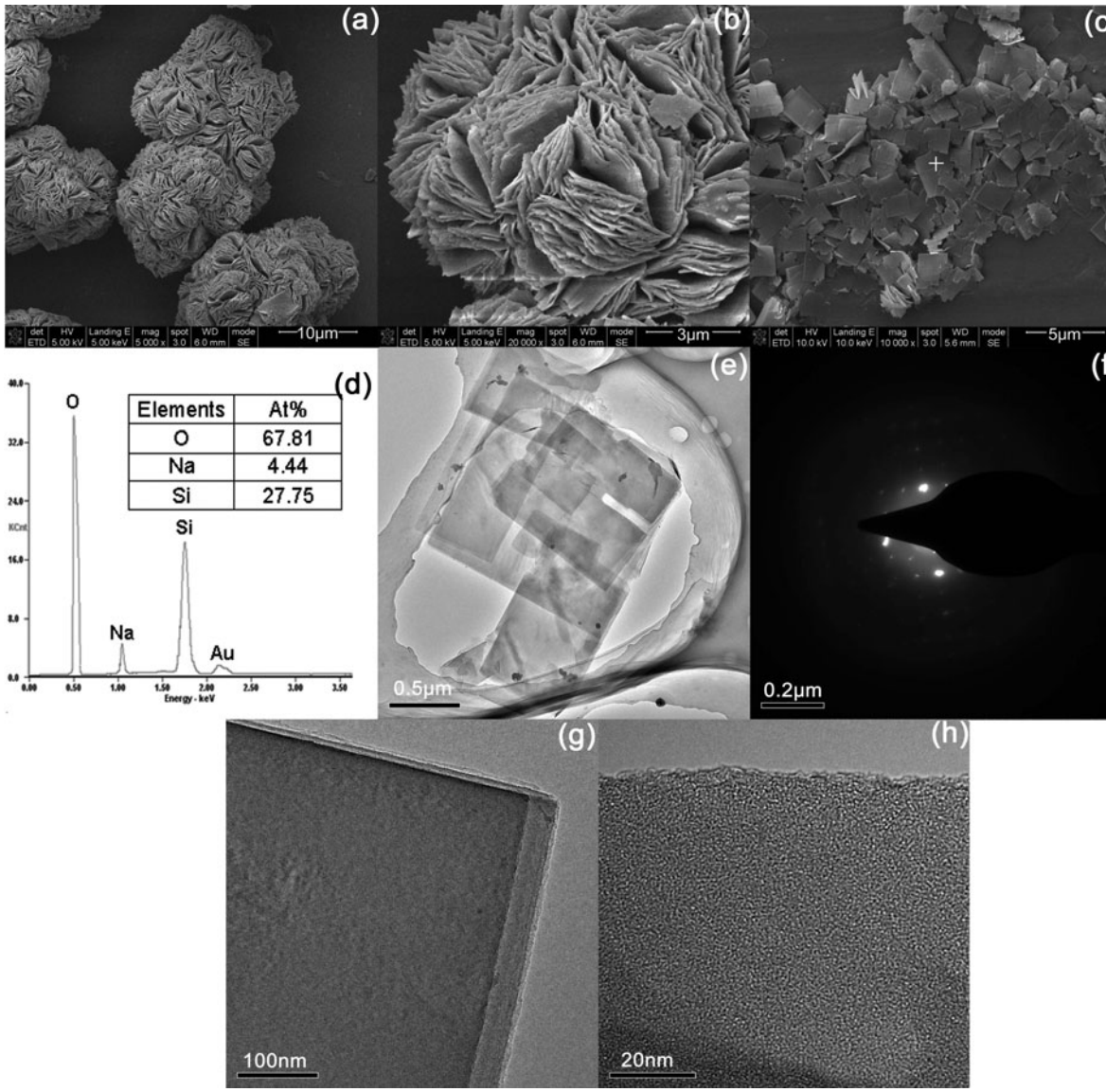

Figure 3. SEM images of C-magadiite (a,b) and P-magadiite (c); (d) EDS of the point marked with a + sign in part c; (e) low-magnification TEM of P-magadiite; and (f) the corresponding SAED pattern; (g,h) HRTEM of P-magadiite showing the edge and internal structures of the mesoporous plates.

magadiite during the testing. The representative HRTEM images of P-magadiite (Figure 3g,h) show the edges and internal structures of the mesoporous plates. The P-magadiite sample has the characteristics of an outer lamellar structure (Figure 3g) and an inner ordered mesoporous structure (Figure 3h). The P-magadiite interlayer distance measured from the outer lamellar structure was 1.6 nm, which is in good agreement with the interplanar spacing obtained from the XRD results (15.6 Å).

The Fourier-transform infrared (FTIR) spectra (Figure 4) show the existence of five-membered rings in the P- and C-magadiite structures. As magadiite is related to hydrous alkali silicates which have multi-layered structures, the vibrational spectra can be divided into two regions, one at 4000−1600 cm^{-1} and the other at 1600−450 cm^{-1}. The region from 4000−1600 cm^{-1} is where the stretching and bending vibrations of water molecules appeared. The two peaks at 3659 and 3584 cm^{-1} are OH-stretching vibrations, ν (OH); and the peak at 1628 cm^{-1} is the water bending vibrations, ν (HOH). The region from 1600−450 cm^{-1} contains the silicate-layer vibrations. The two bands at 1235 cm^{-1} and 1190 cm^{-1} can be assigned to the asymmetric stretching vibration of Si−O−Si, ν_{as} (Si−O−Si). This band was interpreted by Garcés *et al.* (1988) an indication of a five-membered ring in the structure. The band at 1090 cm^{-1} is the terminal Si−O^{-} stretching

https://doi.org/10.1346/CCMN.2013.0610605 Published online by Cambridge University Press

band, ν (Si−O$^-$) (Huang *et al.*, 1999). The bands at 783, 622, 577, and 461 cm^{-1} represent the Si−O−Si symmetric stretching vibration, ν (Si−O−Si). The framework vibrations (at 1235 and 1190 cm^{-1}) indicate crystalline ordering in the magadiite. These bands have been observed in the IR spectra of many zeolites containing five-membered rings with known structures, including silicalite-1 and ZSM-5 (Szostak, 1998). The spectra in Figure 4 support the interpretation of Garcés *et al*. (1988) that the bands at 1235 and 1190 cm^{-1} can be assigned to asymmetric vibrations, ν_{as} (Si−O−Si) of five-membered rings.

The nitrogen adsorption-desorption isotherms and pore-size distributions of C- and P-magadiite (Figure 5) show that the C-magadiite had a small surface area of 28 m^2 g^{-1} and a pore volume of 0.048 cm^3 g^{-1}, whereas for P-magadiite they were 66 m^2 g^{-1} and 0.064 cm^3 g^{-1}, respectively. The inset curves in Figure 5 show the BJH pore-size distribution of the C- and P-magadiite. Both have a relatively narrow distribution with a pronounced peak corresponding to pores with diameters of 4−5 nm. The C- and P-magadiite isotherms have a clearly visible hysteresis loop in the medium relative pressure range (P/P_0 = 0.3−0.8) and in the high-pressure range (P/P_0 = 0.8−0.95) both curves show Type III isotherm characteristics that are typical of mesoporous materials.

Magadiite is often used as an adsorbent, so the ability of the C- and P-magadiite samples to adsorb Ca^{2+} was tested. The Ca^{2+} removal and adsorption capacities of the two samples (Figure 6) were plotted as a function of agitation time. For both samples, the Ca^{2+} concentration in the supernatant dropped rapidly in the first 20 min. The concentration then decreased more slowly until 50 min for P-magadiite (or 70 min for C-magadiite) and then remained constant at longer adsorption times (Figure 6a). The concentration decreased more in the P-magadiite because of its larger BET surface area. The experimental equilibrium and maximum adsorption capacities (q_{max}) for P- and C-magadiite were 25.8 and 21.5 mg g^{-1}, respectively (Figure 6b). The calculated CEC of P- and C-magadiite were 64.5 mmol/100 g and 53.8 mmol/100 g, respectively. The Ca^{2+} exchange capacity of P-magadiite is equivalent to that for

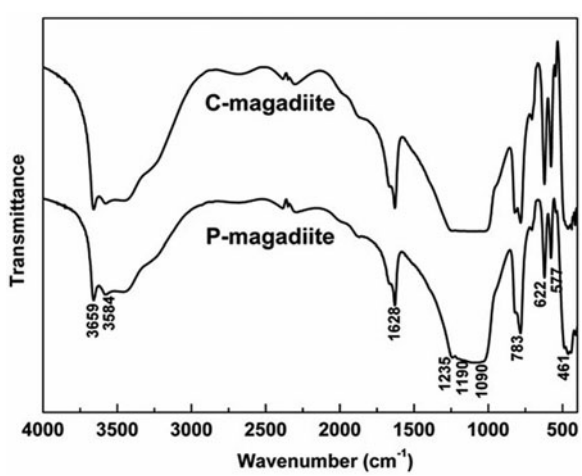

Figure 4. FTIR spectra of C- and P-magadiite.

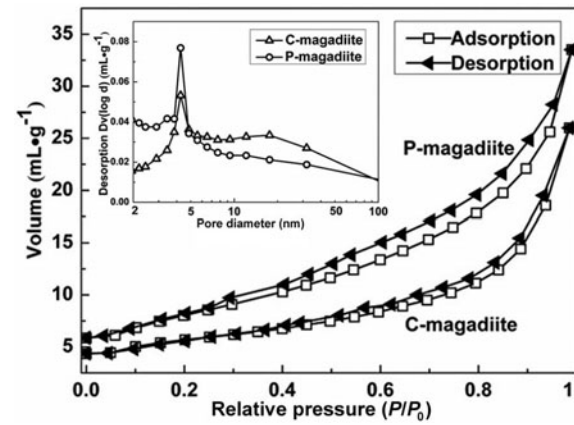

Figure 5. N_2 adsorption-desorption isotherms and pore-size distributions (inset) of C- and P-magadiite.

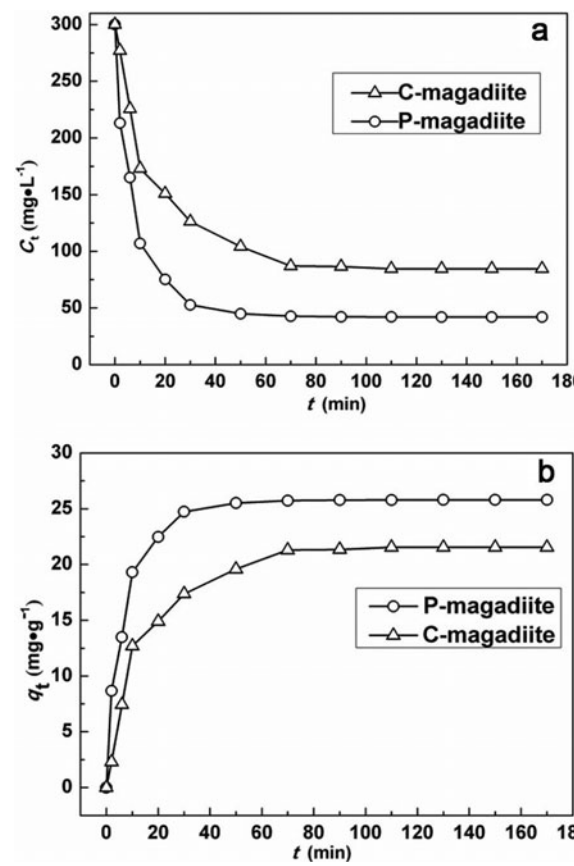

Figure 6. (a) Ca^{2+} removal and (b) Ca^{2+} adsorption capacity *vs.* agitation time, *t*, for C- and P-magadiite. (Ca^{2+} initial concentration, C_0 = 300 mg L^{-1}, magadiite dosage = 2 g L^{-1}, pH = 7.0 ± 0.2, temperature = 298 ± 1 K).

https://doi.org/10.1346/CCMN.2013.0610605 Published online by Cambridge University Press

δ-$Na_2Si_2O_5$ (de Lucas *et al.*, 2002), which suggests that P-magadiite could be used as a builder in detergents. In addition, P-magadiite may be a better choice for preparing magadiite derivative compounds through intercalation, interlayer grafting, and pillaring reactions due to its plate-like shape and greater BET surface area.

CONCLUSIONS

A hydrothermal process for the preparation of plate-like magadiite has been reported. Adding zirconia balls to the hydrothermal solution not only affected the microstructures of the magadiite, but also the yield of the product. Adding the balls promoted the crystallization process by providing a solid−liquid interface for heterogeneous nucleation. The product started to form after 12 h of reaction and the maximum yield reached 52% of the theoretical yield after 72 h. In contrast, when no balls were added, the product did not start to form until after 16 h and the maximum yield was only 45% after 96 h. With no zirconia balls, the magadiite formed by the hydrothermal process had cauliflower-like characteristics with aggregates of thin platelets of ~10−20 μm diameter. With the zirconia balls, the magadiite synthesized contained isolated plate-like shapes, with wafers of 1−3 μm radius, and few aggregates. Both the synthesized P- and C-magadiite contained single Na-magadiite phases with mesoporous characteristics and average pore sizes of 4−5 nm. The P-magadiite had a surface area of 66 $m^2\ g^{-1}$, a pore volume of 0.064 $cm^3\ g^{-1}$, and a Ca^{2+} binding capacity of 25.8 mg g^{-1} for an initial Ca^{2+} concentration of 300 mg L^{-1} at 298 K. These properties show that the P-magadiite could be an ideal adsorbent or pillared material.

ACKNOWLEDGMENTS

The support of the National Natural Science Foundation of China under Grant No. 50972103 and the Scientific Research Foundation for Returned Overseas Chinese Scholars, Ministry of Education of China, is gratefully acknowledged. The authors also thank Dr Jeanne Wynn for improving the English in the manuscript.

REFERENCES

Ágnes, F., Imre, K., Niwa, S.I., Toba, M., Kiyozumi, Y., and Mizukami, F. (1999) Mesoporous materials synthesized by intercalation of silicate tubes between magadiite layers. *Applied Catalysis A: General*, **176**, L153−L158.

Almond, G.G., Harris, R.K., and Franklin, K.R. (1997) A structural consideration of kanemite, octosilicate, magadiite and kenyaite. *Journal of Materials Chemistry*, **7**, 681−687.

Beugster, H.P. (1967) Hydrous sodium silicates from Lake Magadi, Kenya: Precursors of bedded chert. *Science*, **157**, 1177−1180.

Bi, Y., Lambert, J.F., Millot, Y., Casale, S., Blanchard, J., Zeng, S., Nie, H., and Li, D. (2011) Relevant parameters for obtaining high-surface area materials by delamination of magadiite, a layered sodium silicate. *Journal of Materials Chemistry*, **45**, 18403−18411.

Binette, M.J. and Detellier, C. (2002) Lamellar polysilicate nanocomposite materials: Intercalation of polyethylene glycols into protonated magadiite. *Canadian Journal of Chemistry*, **80**, 1708−1714.

Chen, Y., Yu, G., Li, F., and Wei, J. (2013) Structure and photoluminescence of composites based on CdS enclosed in magadiite. *Clays and Clay Minerals*, **61**, 26−33.

de Lucas, A., Rodríguez, L., Lobato, J., and Sánchez, P. (2002) Synthesis of crystalline δ-$Na_2Si_2O_5$ from sodium silicate solution for use as a builder in detergents. *Chemical Engineering Science*, **57**, 479−486.

Díaz, U., Cantín, Á., and Corma, A. (2007) Novel layered organic-inorganic hybrid materials with bridged silsesquioxanes as pillars. *Chemistry of Materials*, **19**, 3686−3693.

Eypert-Blaison, C., Sauzéat, E., Pelletier, M., Michot, L.J., Villiéras, F., and Humbert, B. (2001) Hydration mechanisms and swelling behavior of Na-magadiite. *Chemistry of Materials*, **13**, 1480−1486.

Eypert-Blaison, C., Michot, L.J., Humbert, B., Pelletier, M., Villiéras, F., and d'Espinose de la Caillerie, J.-B. (2002) Hydration water and swelling behavior of magadiite. The H^+, Na^+, K^+, Mg^{2+}, and Ca^{2+} exchanged forms. *The Journal of Physical Chemistry B*, **106**, 730−742.

Fujita, I., Kuroda, K., and Ogawa, M. (2003) Synthesis of interlamellar silylated derivatives of magadiite and the adsorption behavior for aliphatic alcohols. *Chemistry of Materials*, **15**, 3134−3141.

Garcés, J.M., Rocke, S.C., Crowder, C.E., and Hasha, D.L. (1988) Hypothetical structures of magadiite and sodium octosilicate and structural relationships between the layered alkali metal silicates and the mordenite- and pentasil-group zeolites. *Clays and Clay Minerals*, **36**, 409−418.

Guerra, D.L., Ferrreira, J.N., Pereira, M.J., Viana, R.R., and Airoldi, C. (2010) Use of natural and modified magadiite as adsorbents to remove Th(IV), U(VI), and Eu(III) from aqueous media-thermodynamic and equilibrium study. *Clays and Clay Minerals*, **58**, 327−339.

Huang, Y., Jiang, Z., and Schwieger, W. (1999) Vibrational spectroscopic studies of layered silicates. *Chemistry of Materials*, **11**, 1210−1217.

Ide, Y., Ochi, N., and Ogawa, M. (2011) Effective and selective adsorption of Zn^{2+} from seawater on a layered silicate. *Angewandte Chemie*, **50**, 654−656.

Kikuta, K., Ohta, K., and Takagi, K. (2002) Synthesis of transparent magadiite-silica hybrid monoliths. *Chemistry of Materials*, **14**, 3123−3127.

Kooli, F., Mianhui, L., Alshahateet, S.F., Chen, F., and Yinghuai, Z. (2006) Characterization and thermal stability properties of intercalated Na-magadiite with cetyltrimethylammonium (C16TMA) surfactants. *Journal of Physics and Chemistry of Solids*, **67**, 926−931.

Kwon, O.Y., and Park, K.W. (2004) Synthesis of layered silicates from sodium silicate solution. *Bulletin − Korean Chemical Society*, **25**, 25−26.

Lagaly, G. and Beneke, K. (1975) Magadiite and H-magadiite: I. Sodium magadiite and some of its derivatives. *American Mineralogist*, **60**, 642−649.

Macedo, T.S.R., Petrucelli, G.C., and Airoldi, C. (2007) Silicic acid magadiite as a host for n-alkyldiamine guest molecules and features related to the thermodynamics of intercalation. *Clays and Clay Minerals*, **55**, 151−159.

Mallouk, T.E. and Gavin, J.A. (1988) Molecular recognition in lamellar solids and thin films. *Accounts of Chemical Research*, **31**, 209−217.

Nunes, A.R., Moura, A.O., and Prado, A.G. (2011) Calorimetric aspects of adsorption of pesticides 2, 4-D, diuron and atrazine on a magadiite surface. *Journal of Thermal Analysis and Calorimetry* , **106**, 445−452.

Pastore, H.O., Munsignatti, M., and Mascarenhas, A.J.S.

(2000) One-step synthesis of alkyltrimethylammonium-intercalated magadiite. *Clays and Clay Minerals*, **48**, 224–229.

Schwieger, W. and Lagaly, G. (2004) Alkali silicates and crystalline silicic acids. Pp. 541–551 in: *Handbook of Layered Materials* (S.M. Auerbach, K.A. Carrado, and P.K. Dutta, editors). Monograph **11**, Marcel Dekker Inc, New York.

Sprung, R., Davis, M.E., Kauffman, J.S., and Dybowski, C. (1990) Pillaring of magadiite with silicate species. *Industrial & Engineering Chemistry Research*, **29**, 213–220.

Supronowicz, W., Roessner, F., Schwieger, W., Meilikhov, M., and Esken, D. (2012) Synthesis and properties of Sn-containing magadiite. *Clays and Clay Minerals*, **60**, 254–264.

Szostak, R. (1998) *Molecular Sieves (second edition)*. Blackie Academic & Professional, Glasgow, UK.

Takahashi, N. and Kuroda, K. (2011) Materials design of layered silicates through covalent modification of interlayer surfaces. *Journal of Materials Chemistry*, **21**, 14336–14353.

Wang, Y.R., Wang, S.F., and Chang, L.C. (2006) Hydrothermal synthesis of magadiite. *Applied Clay Science*, **33**, 73–77.

Zhang, Z., Saengkerdsub, S., and Dai, S. (2003) Intersurface ion-imprinting synthesis on layered magadiite hosts. *Chemistry of Materials*, **15**, 2921–2925.

(*Received 13 August 2013; revised 2 December 2013; Ms. 801; AE: S.M. Kuznicki*)